Tuner Effect on the Field Flatness of SNS Superconducting RF Cavity

Sun An
Oak Ridge National Laboratory, Oak Ridge, TN 37830, USA
Haipeng Wang
Jefferson Lab, Newport News, VA 23606, USA

Abstract

The field flatness in a multi-cell superconducting cavity affects not only the net accelerating voltage, but also the peak surface field in each individual cell [1]. Our measurement indicates that the field flatness changes the Q external of the Fundamental Power Coupler (FPC) and the Q external of the Field Probe (FP). The field amplitude tilts linearly to the distance between the cell center and the cavity's geometry center (pivot point). The tilting rate has been measured in a cryomodule cold (2K) test, being about 2% per 100 KHz, relative the field flatness at the cavity's center frequency of 805MHz. The bead pulling measurements confirmed that the field flatness change is 2.0% per 100 KHz for a medium β cavity with the helium vessel, and 1.72% per 100 KHz without the helium vessel. The simulations (ANSYS and SUPERFISH) further confirmed this change rate. The detail investigation reveals that the longitudinal capacitive gap's deformation is the main cause of the frequency change. The field flatness change was not only due to the uneven stored energy change within the cell, but also due to the cell-to-cell coupling. The field flatness change due to the tuner effect finally can be estimated based on these data.

I. Introduction

The Spallation Neutron Source (SNS) to be built at Oak Ridge National Laboratory (ORNL), TN, uses the superconducting RF cavities to accelerate H- ions in from the 185MeV after RFQ linac to the final energy of 1GeV. It is intended to deliver a proton beam of up to 1.4 MW power to a mercury target for neutron spallation [2-4]. Two types of 6-cell Niobium cavities are used in the superconducting linac: 33 β=0.61 cavities and 48 β=0.81 cavities.

SNS specification for both high beta and low beta production cavities on the field flatness is 8%. The only checkpoint is by the bead-pulling measurement after the cavity is welded into the helium tank. After the final Buffer Chemical Polishing (BCP), there is no way to check or correct the field flatness problem once it is in the cryomodule string assembly stage. Is the field flatness more than 8% or not? How much could it affect the Q externals of FPC and Field Probe? They are important questions to be concerned.

The cavity tuner's frame sites on the FP end to compress the end dish of the cavity against to the helium vessel. All the mechanics operates at near the 2K. The frequency tuning range is about ±245kHz around 805MHz. Total axial compression range is about 1.8mm.

From our initial study, we found that while the tuner changes the cavity resonance frequency, it also changes the cavity's field flatness and Q external of the couplers. In principle, the field flatness changes not only the maximum integrated accelerating voltage, but also the peak surface field in each individual cell. When the peak surface field in the end cell is changed, the power coupling to the coupler is also changed. If a cavity has been qualified in a vertical test (VTA) on the specification, it reached the 94% of maximum surface magnetic filed for the quench or of maximum surface electric field for the on-set field emission. It could be failed in the cryomodule test (CMTF) just due to the additional 7% of field flatness change in the assembly process. So the field flatness is an important variable parameter and need to be controlled in the cavity production process.

In this paper, first we investigated cavity FPC and Field Probe Q external change, when the tuner moved from low limit to high limit in the cryomodule test (CMTF) at 2K's temperature. This change could be well characterized as the field tilt change from one direction to the other. Second the bead-pulling measurements were carried out in our production tuning area using their existing setup. The result confirmed field tilt rate of 2% per 100 kHz obtained from the CMTF. Third we combined simulation techniques by using the ANSYS code for the mechanical displacement of the cavity shape and by using the SUPERFISH code for the electromagnetic properties, to analyze the net cavity volume change when the tuner move, and applied it into to the perturbation theory. The field flatness change due to the cell-to-cell coupling can be concluded. Finally we use the analysis results to predict a cavity's filed flatness change in a cryomodule at 2K, assuming the pump-down and cool-down processes do not change the cavity field flatness.

The original definition of the N-cell cavity field flatness is

$$\eta_{ff} = \frac{V_{c\max} - V_{c\min}}{\frac{1}{N}\sum_{i=1}^{N} V_{ci}} \times 100\% \cdot \qquad (1)$$

Here V_{ci} is the accelerating voltage of the ith cell. $V_{c\max}$ and $V_{c\min}$ is the maximum and minimum cell voltage in the cavity, respectively.

For a fixed $\beta=v/c$ structure, all the cells in the cavity have an equal accelerating gap $d=\beta c/(2f_0)$. Here the c is the speed of light, f_0 is operating frequency. The cell's accelerating voltage is $V_c = E_c\int_0^d f(z)\cos(\pi\frac{z}{d}+\phi_0)dz = E_cT(d)$. Here E_c is the peak axial electric field along the beam axis z. The $f(z)$ is the field distribution function. As long as the cavity shape and the gap d don't change from cell to cell, or a small perturbation change which only changes the E_c but not $f(z)$ and d. So the transit time factor $T(d)$ will be a constant. Then the equation (1) becomes:

$$\eta_{ff} = \frac{E_{c\max} - E_{c\min}}{\frac{1}{N}\sum_{i=1}^{N} E_{ci}} \times 100\% \tag{2}$$

The equation (2) shows that the field flatness η_{ff} doesn't depend on the cavity frequency, and doesn't change either if the E_{ci} in every cell's changes in a same ratio.

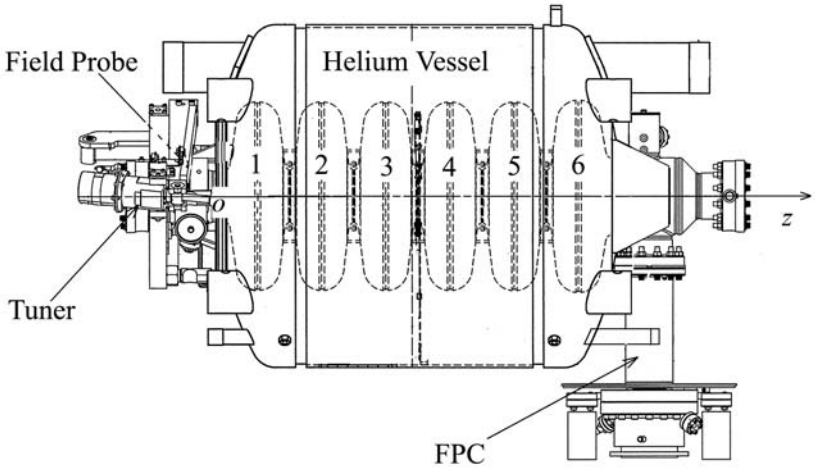

Figure 1: The SNS medium β cavity. The tuner frame is to be installed on the FP side. We follow above convention that the cell 1 is the FP end cell and the cell 6 is the FPC end cell.

II. Measurement in the cold cryomodule at 2K

The SNS FPC and Field Probe are both electric antenna type couplers located on opposite ends of the cavity (fig.1). The Q external can be expressed [5] as:

$$Q_{ext} = \frac{2C_s}{\varepsilon_0} \frac{\int_V \mathbf{E}^2 dv}{(\int_S \mathbf{E} \cdot d\mathbf{S})^2} . \tag{3}$$

Here the C_s is the coupler's probe self capacitance plus any parasitic capacitance. It depends on the probe position near the cavity and depth penetrating into the beam pipe. **E** is the cavity electric field. The volume integration is over the cavity volume, and the area integration is over the probe area. The equation (3) could be approximately expressed as following:

$$Q_{ext} = K \frac{U}{E_{ce}^{\ 2}} . \tag{4}$$

Here K is a constant, if the $\int_S \mathrm{E} \cdot d\mathrm{S}$ can be separated into $\int_S \mathbf{E} \cdot d\mathbf{S} = E_{ce} \int_S f(s) ds$,

$K = \dfrac{4C_s}{\varepsilon_0{}^2\left[\int_S f(s)ds\right]^2}$. $U = \dfrac{1}{2}\varepsilon_0\int_V \mathbf{E}^2 dv$ is the cavity total stored energy without time average. The equation (4) indicates that the Q_{ext} will not change, if U/E_{ce}^2 keeps a same ratio.

In reality, we did observe the Q external variation just due to the tuner move. We exclude this change might caused by the instability of the helium pressure and thermal unbalance in the cryomodule system. That means there must be an U/E_{ce}^2 change. If the field level or the total stored energy U is same, there must be an E_{ce} change or a field flatness η_{ff} change after the tuner motion.

The measurement was done on the medium β M01 production cryomodule in CMTF. After the cavity cooled down to 2K, a low power scattering parameter S21 (by two-port network analyzer from FPC to FP) was measured. By measuring the S21's –3dB bandwidth, we can get the Q_{load} of the cavity. That includes cavity's intrinsic quality factor Q_0, the FPC's Q external Q_{extFPC} and Field Probe's Q external Q_{extFP}:

$$\frac{1}{Q_{load}} = \frac{1}{Q_0} + \frac{1}{Q_{extFPC}} + \frac{1}{Q_{extFP}} \tag{5}$$

Known that the Q_{extFPC} is about 7.3×10^5, Q_0 is approximately 1×10^{10} and Q_{extFP} equals about 1.7×10^{12} for SNS cavity, so $Q_{load} \approx Q_{extFPC}$ can be used to determine the Q external change on the FPC. The power transmission loss at cavity resonance is [6]:

$$S21 = 10\cdot\log\left[\frac{4\beta_1\beta_2}{(1+\beta_1+\beta_2)^2}\right] \quad \text{[dB]} \tag{6}$$

Here $\beta_1 = Q_0/Q_{extFPC}$ and $\beta_2 = Q_0/Q_{extFP}$ are the coupling coefficient of the FPC and fo the FP, respectively. From above known Qs' order, the Q_{extFP} can be simplified and measured by:

$$Q_{extFP} = 4Q_{extFPC}\cdot 10^{\frac{|S21|}{10}} \tag{7}$$

For an absolute Q_{extFP} value, one needs to calibrate the instrumentation circuit including preamplifier and cables. A relative measurement to the center frequency's values can be used.

$$\frac{Q_{extFP}}{Q_{extFP0}} = \frac{Q_{extFPC}}{Q_{extFPC0}}\cdot 10^{\frac{|S21-S21_0|}{10}} \tag{8}$$

Here note 0 represents the corresponding values at f_0=805MHz.

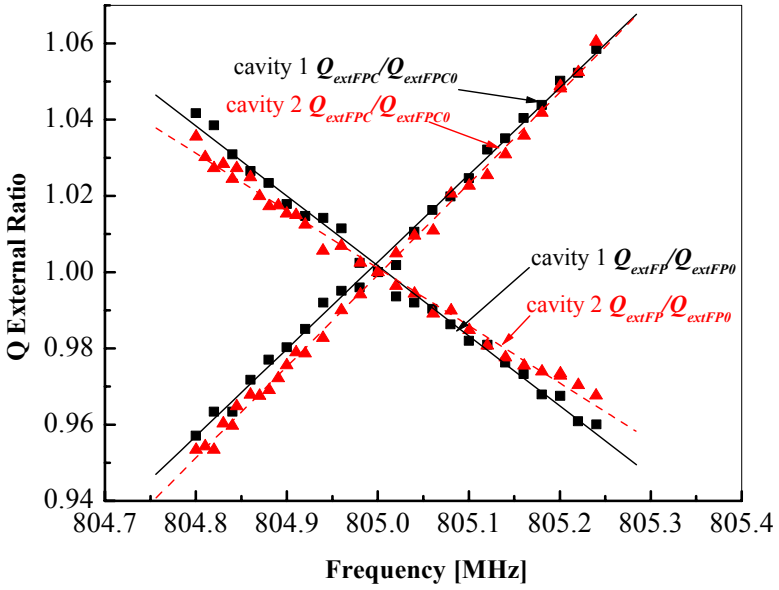

Figure 2: The FPC and FP Q externals change relative to the center frequency's values. Here Q_{extFPC} and Q_{extFP} are the FPC and FP Q externals at tuner-tuned frequencies, respectively. The data lines are linear fittings.

The equation (4) yields:

$$\begin{cases} E_{cFPC} = E_{cFPC0}\sqrt{Q_{cFPC0}/Q_{cFPC}} \\ E_{cFP} = E_{cFP0}\sqrt{Q_{cFP0}/Q_{cFP}} \end{cases} \tag{9}$$

The equation (9) and Figure 2 indicate that the field amplitude decreases at the FPC-end cell and increases at the FP-end cell, when the cavity frequency increases. This trend happens when the tuner stretching the cavity. Supposing the cavity field flatness is perfect at operation frequency of 805MHz, i.e., η_{ff}=0, and the electric field tilts as uniformly as the linear fitting illustrated in the Figure 2, the field flatness can be expressed as:

$$\eta_{ff} = \frac{\left|\sqrt{Q_{cFPC0}/Q_{cFPC}} - \sqrt{Q_{cFP0}/Q_{cFP}}\right|}{\sqrt{Q_{cFPC0}/Q_{cFPC}} + \sqrt{Q_{cFP0}/Q_{cFP}}} \times 200\% \tag{10}$$

As shown in Figure 3, the field flatness change in this example is about 2% per 100 KHz around operation frequency.

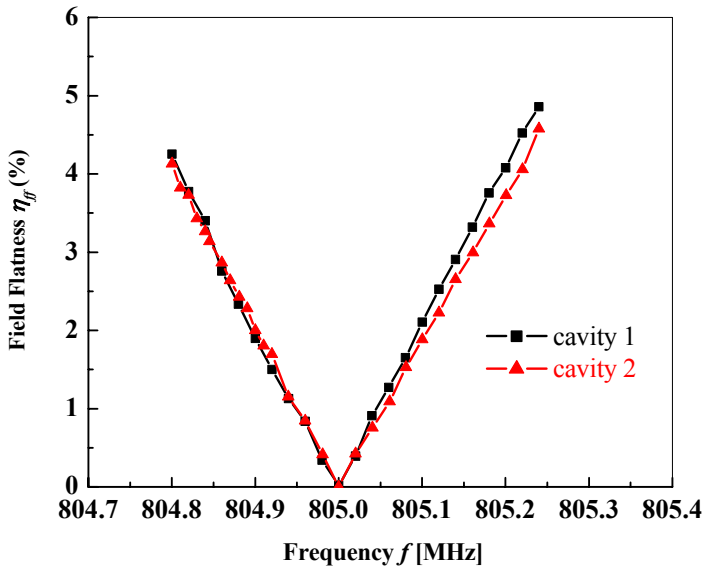

Figure 3: Measured field flatness changes of the cavity 1 and cavity 2 on the SNS medium β cryomodule M02 as the function of tuner-tuned cavity frequencies.

III. Bead-pulling Measurement

To verify this result from the cryomodule test, we did two bead-pulling measurements to measure the axial electric field profiles on the SNS medium β cavity MB-19 with helium vessel and on the cavity MB-29 without helium vessel. The tuners were installed to tune the cavities. The Figure 4 shows the measurement setup.

Figure 4: Bead-pulling setup to measure the field flatness of SNS MB-19 with Helium Vessel.

A 3mm long syringe needle on the pulling string was sent through the cavity center axis. If we neglect the on-axial magnetic field H_Φ, the cavity's stored energy perturbed by the small metallic cylinder is (exclude the 1/2 time average factor) [7]:

$$\Delta U(z) = -\frac{1}{2}\varepsilon_0 E_z^{\,2}(z)\pi a^2 d\left[1-\frac{\pi^2}{2}\left(\frac{a}{\lambda_0}\right)^2\right] \tag{11}$$

Here $E_z(z)$ is the on-axial electric field at position z. a is the needle radius, d is its length. For $a<<\lambda_0$ of the wavelength of f_0=805MHz, the second term of the equation (11) can be neglected. According to the perturbation theory:

$$\frac{\Delta U(z)}{U} = -\frac{\Delta f(z)}{f_0} \tag{12}$$

Here U is the cavity total stored energy without the bead's perturbation and excluding the 1/2 time average factor. Defining Δf_i as the maximum frequency change in the ith cell, we find that:

$$E_{ci}^{\,2} = k\Delta f_i \tag{13}$$

The k can be found out that it is the constant of bead and cavity geometry dimensions dependent only. The field flatness η_{ff} of the N-cell cavity is

$$\eta_{ff} = \frac{\sqrt{\Delta f_{\max}} - \sqrt{\Delta f_{\min}}}{\frac{1}{N}\sum_{i=1}^{N}\sqrt{\Delta f_i}} \times 100\% \tag{14}$$

In the experiment, we did not directly measure the frequency change $\Delta f(z)$. Instead we measure the phase angle of scattering parameter of S21 by a network analyzer. Record the change of **arg**(S21) as the bead pulling through the cavity (distance z change). We can write the S21 as the function of drive frequency f.

$$S21(f) = \frac{2\sqrt{\beta_1\beta_2}}{(1+\beta_1+\beta_2)+i\Omega(f)} \tag{15}$$

$$\Omega(f) = Q_0\left(\frac{f}{f_0}-\frac{f_0}{f}\right) \tag{16}$$

Here β_1 and β_2 are the coupling coefficients of input and output couplers. We found out by a carefully setting up the system with weak couplings $\beta_1<<1$ and $\beta_2<<1$, a preamplifer on the pickup coupler, and the shortest the needle length d. We can satisfy the condition of $2Q_L\Delta f << f_0$, here $Q_L=Q_0/(1+\beta_1+\beta_2)$. That is to control the arg(S12) within a few degrees.

$$\arg(S12)(z) = \arctan\left(-2Q_L\frac{\Delta f(z)}{f_0}\right) \approx -2Q_L\frac{\Delta f(z)}{f_0} \qquad \text{[radian]} \tag{17}$$

In this case, the perturbed frequency change is proportional to the S12's phase angle change.

So the field flatness can be calculated by:

$$\eta_{ff} = \frac{\sqrt{-\arg(S12)_{\max}} - \sqrt{-\arg(S12)_{\min}}}{\frac{1}{N}\sum_{i=1}^{N}\sqrt{-\arg(S12)_i}} \times 100\% \tag{18}$$

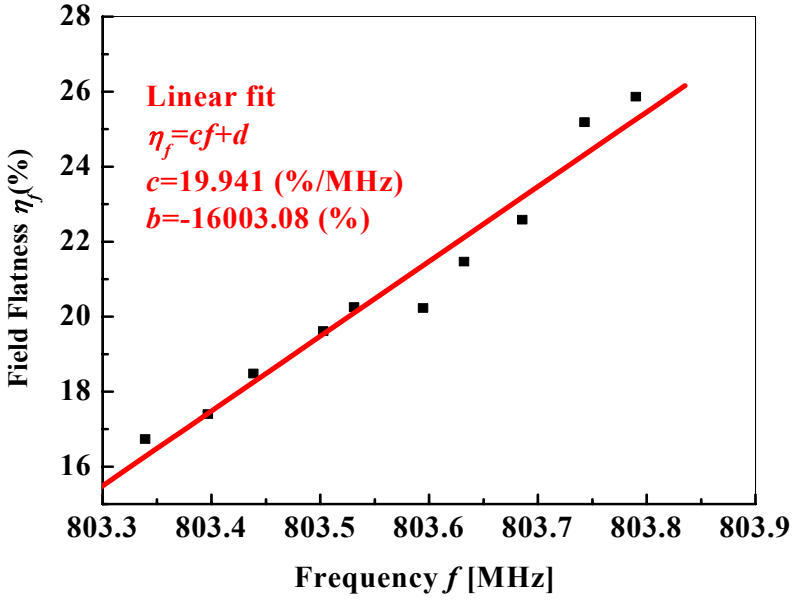

Figure 5: The MB-19 cavity's (with helium vessel) field flatness measured by the bead pulling. The initial field flatness was 26% before the tuner compressed the cavity.

As illustrated in Figure 5, the field flatness change is linear to the cavity frequency, and its rate is also about 2% per 100 KHz. This result agrees with the cryomodule measurement.

The bead-pulling result confirmed that the electric field amplitude decrease at the FPC-end cell, and increase at the Field Probe-end cell, when the cavity is tuned to increase the resonance frequency, as shown in Figure 6. The field amplitude changing rates at both end cells were larger than at center cells. The measurement result of the MB-29 cavity without a helium vessel was similar to the MB-19 cavity, but the field flatness change was ~1.72% per 100 KHz. We concluded the cause probably due to the MB-29 was a free cavity.

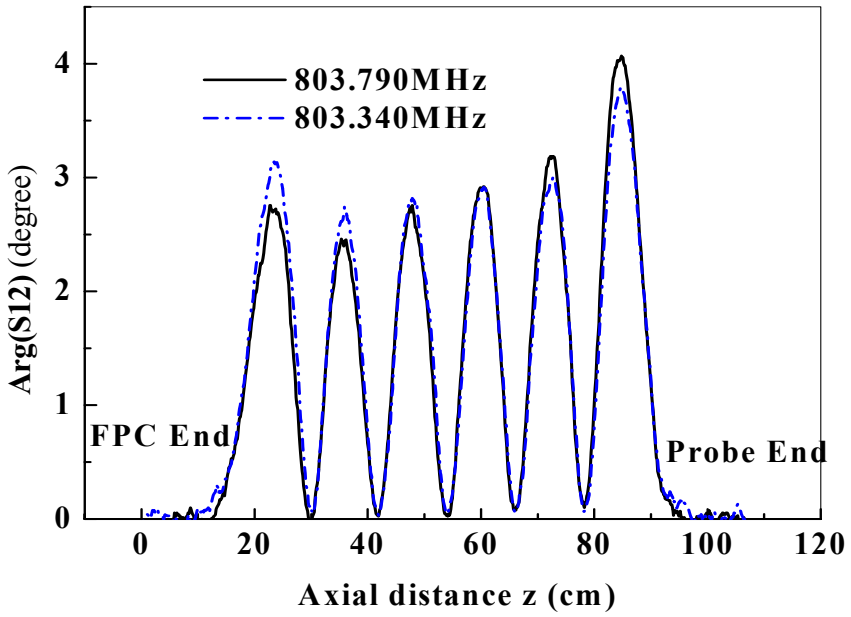

Figure 6: The measurement of bead pulling on MB-19 cavity to measure the electric stored energy profile along the cavity beam axis.

IV. The Finite-Element Codes Simulations

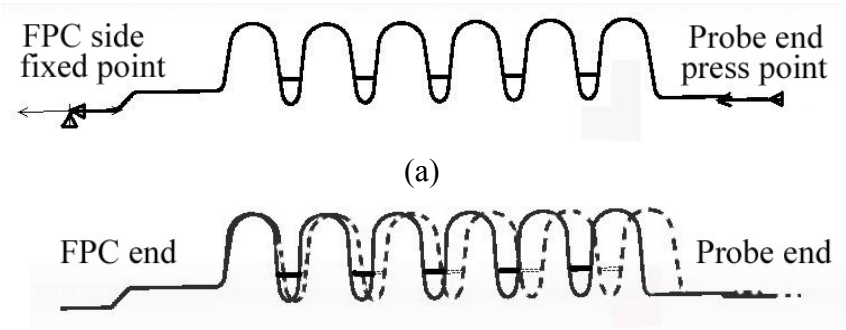

Figure 7: The SNS medium β cavity ANSYS simulation model. (a) The choice of constrain points deferred from two end dishes on the real cavity makes a very small difference in the shape displacement. (b) Exaggerated cavity deformation demonstrated by ANSYS (the dash line is the free shape, and the solid line is the deformed shape).

For a further understanding to the field flatness change mechanism, the ANSYS code was first used to calculate the cavity shape displacement when the tuner compression force is

applied on. A simplified model is showed in Figure 7. Within the tuner's longitudinal motion of ±1.0mm, the niobium cavity deforms only elastically. The cavity shape, wall thickness and reinforce rings are only relevant constrains. The actual displacement of the cavity shape and unloaded cavity shape were inputted into the SUPERFISH code. Using the mesh modification option "ModT36=1" in the AUTOMESH program, the SUPERFISH can calculate newly tuned cavity resonance frequencies and new field distributions.

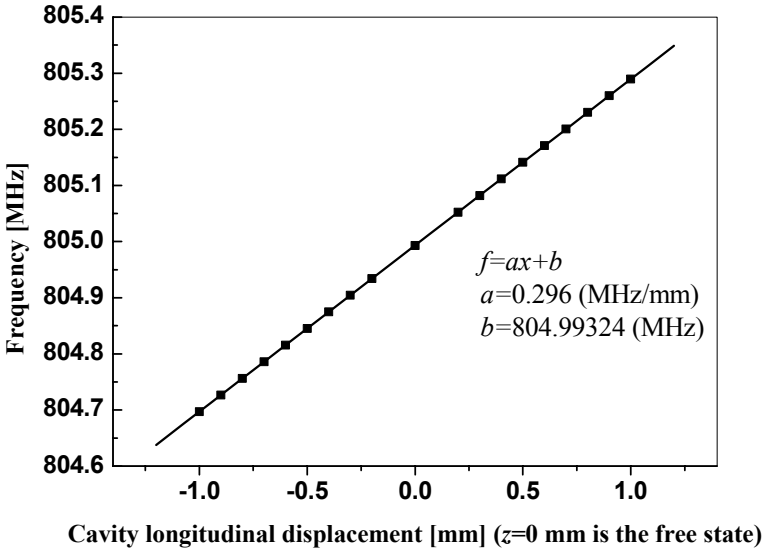

Figure 8: ANSYS and SUPERFISH simulations to the SNS medium β cavity TM010 π mode frequency change versus the cavity longitudinal displacement length, z=0 mm is the free state. The line data is the linear fitting.

As demonstrated in Figure 8, the cavity's frequency change is a linear to the cavity longitudinal displacement within the elastic deformation. The coefficient a is 296 kHz/mm. The same coefficient from the bead-pulling measurement is about 276 kHz/mm. Comparing the Figure 6 with Figure 9, we found that the simulation results on the tuning sensitivity and the field tilt agree with the measurement results both from the CMTF and bead-pulling.

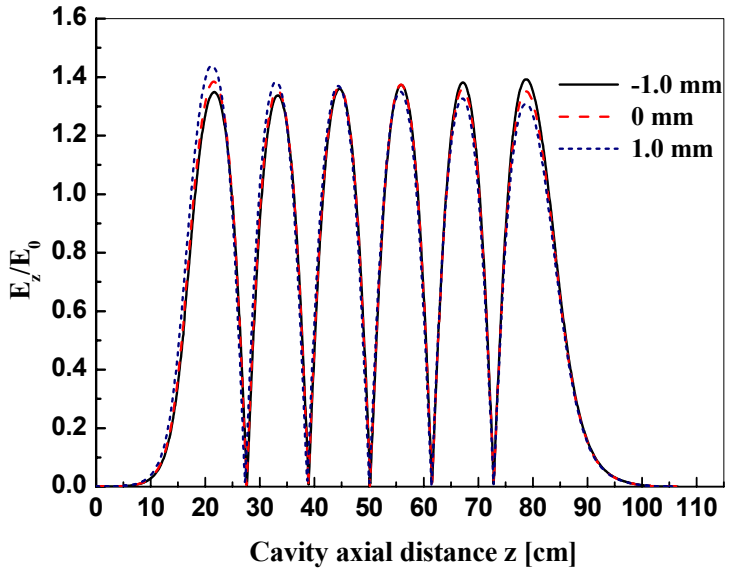

Figure 9: SUPERFISH simulation shows cavity's on-axis electric field amplitude relative changes in three states. 1.0 mm compressed, 0 mm free, and –1.0 mm stretched. Here E_0 is the normalized electric field set in all SUPERFISH runs. Left side is the FPC end, and right side is the Field Probe end.

The original field flatness was defined for a global cavity field characterization; the relative field amplitude change was from cell to cell and normalized to the mean value of all cells. To study the relative field amplitude change within the individual cell and to further explore the cell-to-cell coupling effect, we use the ratio of perturbed field amplitude E_c to its original value at a given frequency E_{c0} (for example, at 805MHz, or at a given tuner position). The Figure 10 shows the simulation results after this re-normalization. The end cells have relatively larger change rates than the center cells. Also note that the change direction, the cell 3 has nearly no change during the frequency change in this example run. If the field flatness is prefect flat at the original reference point, we should see all lines in Figure 10 intercept at a single point. This point should be at, for example, E_{ci}/E_{ci0}=1.0 and f=805MHz. Unfortunately, The initial field flatness in the setup of Figure 10's simulations was about 2%. It depended on the original cavity geometry inputs, mesh densities and constrain parameters on both ANSYS and SUPERFISH programs.

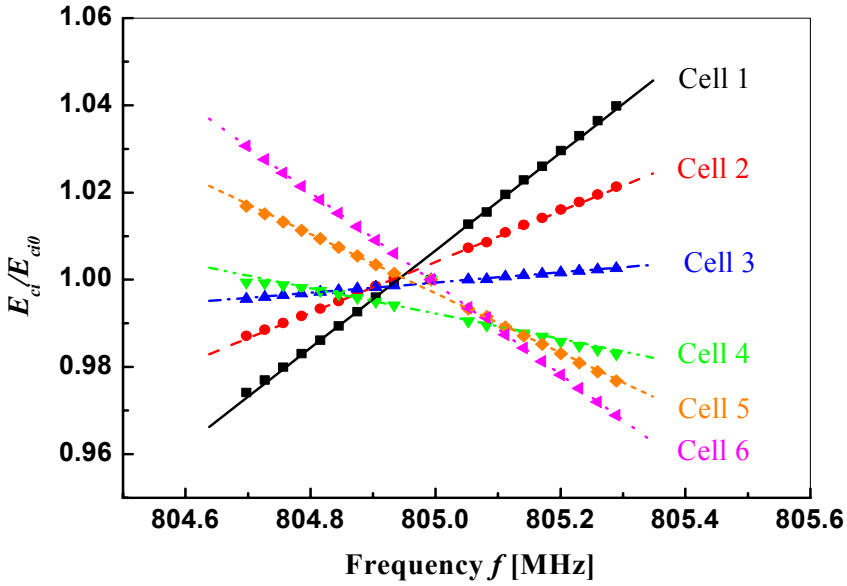

Figure 10: The relative field amplitude change within each individual cell simulated by the ANSYS and SUPERFISH. Here the normalization to the E_{ci0} is at the ith cell and at the operation frequency of 805MHz. The lines are linear fittings for each individual cell.

We can conclude from Figure 10 that the relative field amplitude E_{ci}/E_{ci0} is also linearly frequency depended. The coefficient $\xi(i)$ must be the cell's number depended. The variation range of the interception points in the Figure 10 represents the initial about 2% of field flatness in the simulation setup. We can write the relationship as:

$$E_{ci}/E_{ci0} = \xi(i) f + \eta_i \,, \tag{19}$$

here the η_i is a constant depended on the cell number.

As depicted in Figure 11, the coefficient $\xi(i)$ as the function of the cell's number is a linear relationship. The $\xi(i)$ change range from –0.11 to 0.11 [1/MHz] is also the indication of the field flatness change rate of ~2% per 100 kHz. The linear fitted line also represents the field tilt relative to a flat field distribution. The tilt pivot point, as shown in the Figure 11, is not at the center of any cell. Instead it locates at the structure center. In this simulation case, it is at the position of cell =3.4, because the beam pipe at the FP end (left) is longer than the one at the FPC end (right).

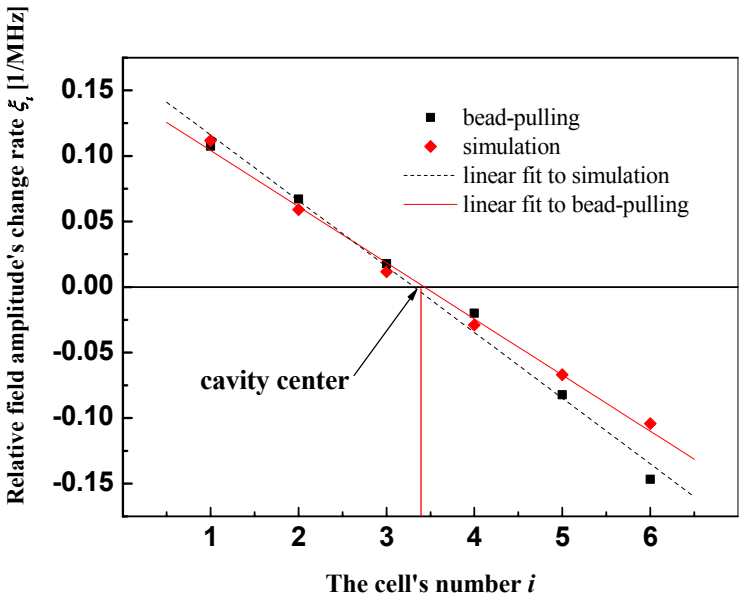

Figure 11: The relative electric field amplitude change within the cell as the function of the cell's number. The slop angle represents the field tilt rate. The negative slop represents the cavity is in the stretching state when the electric field at the cell 1 (Field Probe end) increases.

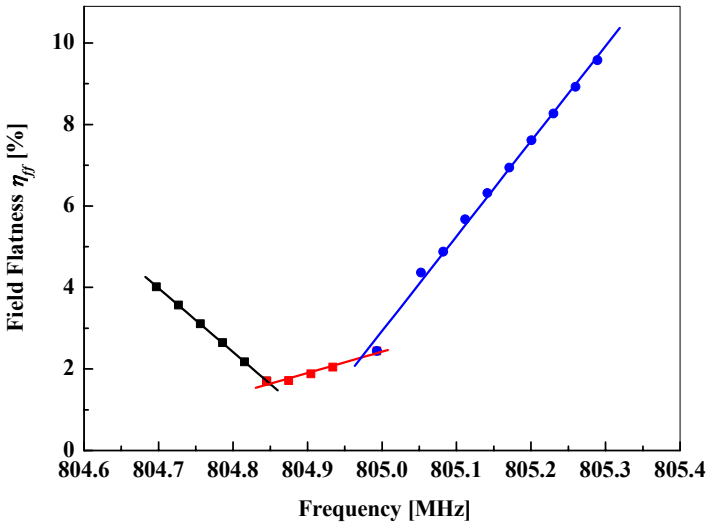

Figure 12: The simulation results of field flatness change with tuner-tuned frequency. The initial field flatness at free state is 2.2% at the frequency of 805 MHz.

If we use the original field flatness definition, we still can plot the simulation result in

Figure 11 into Figure 12. Unlike the measured curves at the CMTF in Figure 3, the curve in the Figure 12 doesn't have the symmetrical "V" shape. The only conclusion from above analysis is that the initial field flatness was not zero. We expect that the symmetry will come back when we can "tune" the simulation input geometry to get an initial field prefect flat. The bead-pulling result has the same problem because the initial field flatness was about 26% and at the high percentage of un-flatness before the tuning.

To study the cavity iris coupling effect on the cell's electric field amplitude when the tuner is compressing the cavity, we used the ANSYS APDL (also by an Excel spreadsheet) to calculate the cavity volume deformation Δv as the function of cavity's axial distance z. As shown in Figure 13, we defined the signs of deformation and volume change. To calculate the cavity deformation correctly, the longitudinal displacement relative to the reference plans has to be properly counted. The longitudinal displacement=(new z – old z) at equators, the longitudinal deformation=(new z – old z – displacement). So at the reference planes, the deformations=0.

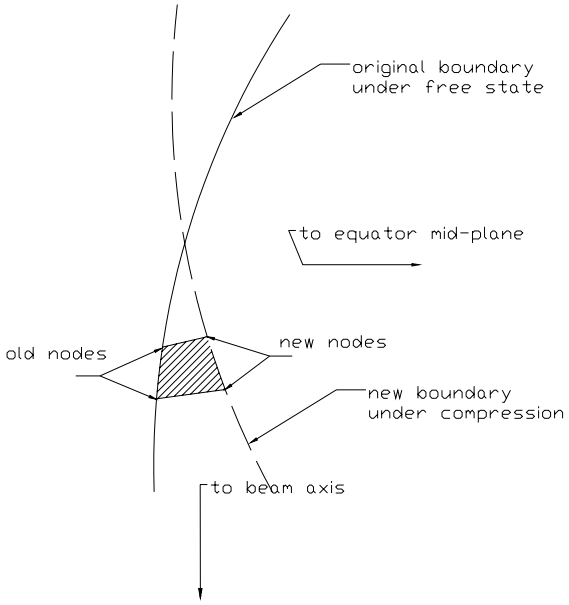

Figure 13: The cavity deformation definition when tuner compresses the cavity from left to right. Every cell's equator mid-plane is longitudinal reference plane, and the beam axis is the transverse reference line. If new nodes move to equator plane, its deformation is positive, otherwise is negative in the longitudinal direction. If new nodes are farer from the beam axis, its deformation is negative, otherwise is positive in the transverse direction. If the volume change makes the cavity cell smaller, the volume change is negative, otherwise is positive.

The calculated results show in Figure 14. The longitudinal displacement is much larger

than the transverse's one. Major longitudinal deformation is near the cavity irises. Major transverse deformation is around equators. Total volume change within the cell arises from the longitudinal deformation change mainly. After calculating the cavity volume change, we integrated it with the electric and magnetic energy densities on the wall (before the mechanical compression) imported from SUPERFISH. The relative stored energy changes in each cell can be obtained. Figure 15 shows this result and compares with the relative electric field amplitudes.

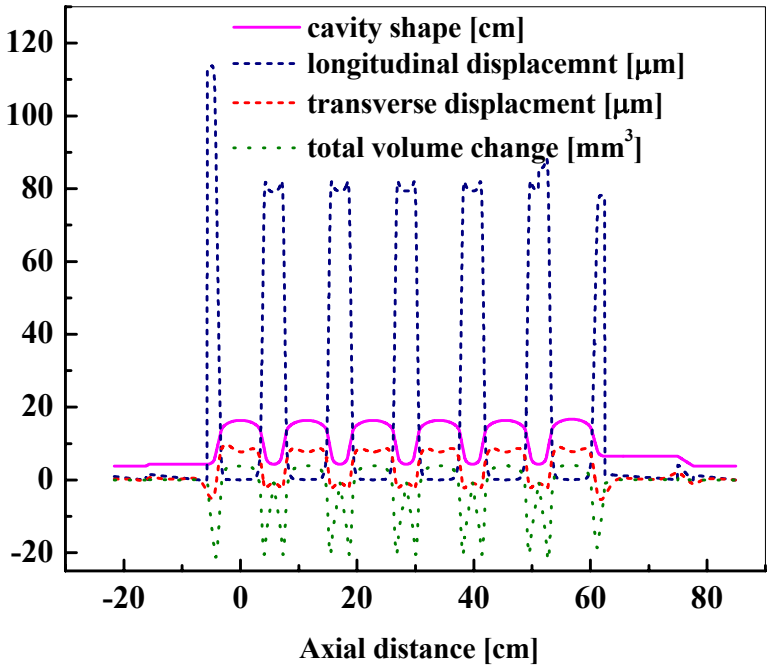

Figure 14: Cavity deformation calculated by ANSYS under a 1.0 mm longitudinal compression. The sign convention follows in Figure 13.

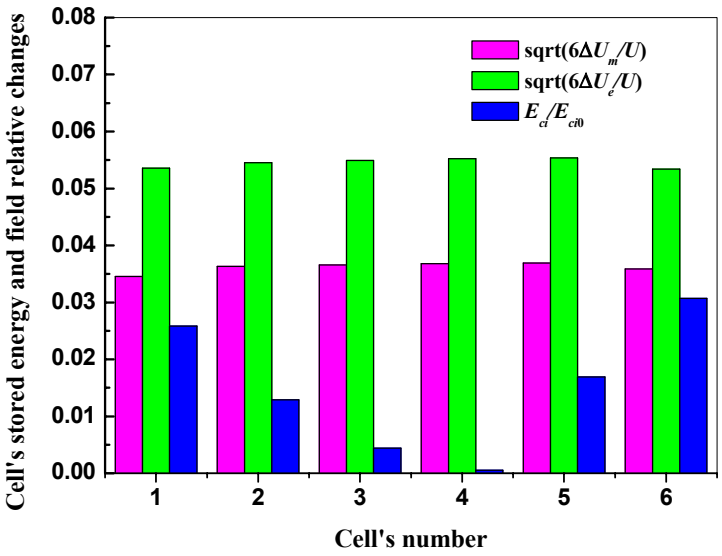

Figure 15: Cavity cell's electric ΔU_e and magnetic ΔU_{m} stored energy changes by cavity deformation after tuner longitudinally compressed 1.0 mm. Here U is the cavity's total stored energy before the compression at 805MHz. E_{ci0} is the cell's maximum amplitude of on-axis electric field in axial direction at 805MHz.

The Figure 15 indicates that if we treat a multi-cell cavity as the individual uncoupled cavity cells, the relative stored energy changes by the volume deformation, both electric and magnetic, are not mainly responsible for the tilt or flatness of the cavity field. Instead cell-to-cell coupling plays a major role in the field tilting or from the flatness. The sum of all cell's differences between the electric and magnetic stored energies is partially responsible for the cavity frequency change, according to the perturbation theory.

V. Guideline to the Cavity Tuning Process

Based on our analysis above, we can use equation (19) to estimate the cavity field flatness change due to the tuner's function. For example, for M021 (MB-05), the field flatness is 7.38% at 804.364MHz, at room temperature before string assembly; the final field flatness could be 4.26% in the 2K cryomodule at the operation frequency of 805MHz. This change only accounted the tuner preload function and tuner moves into the operation position. We did not conclude such changes due to the helium vessel pump down and cool down processes.

To correct this known field flatness change, we can intentionally over tune the field tilt in the opposite direction, during the cavity tuning process, to compensate the titling due to the tuner preload and move-in at the operation position.

VI. Conclusion

The SNS 6-cell cavity has a field flatness tilting effect when the tuner compresses the cavity to tune the cavity frequency. The tilt rate is about 2% per 100 kHz, causing the FPC side's field going up and the Field Probe side's field going down. The tuning sensitivity is about 296 kHz/mm. The Q external measurement at 2K's cryomodule and the field flatness measurement at room temperature's bead pulling have confirmed these results. Detail ANSYS and SUPERFISH simulation results agrees with these experiments and further reveals the mechanism of the field tilt and frequency tuning. The field flatness change is not mainly due to the uneven cell's stored energy change, but due to the cell-to-cell coupling changes. The cavity frequency change is due to the both.

Acknowledgements

The author would to thank R. Overton help us to do the bead-pulling measurements setup. Thanks also go to S. Henderson, J. Galambos, R. Fuja, D. Stout, S. Kim, D-O. Jeon, I. Campisi, M. Champion, and Y. Kang from ORNL and G. Wu, J. Probe, E. Daly, J. Henry, T. Powers, M. Drury, G. Davis, L. King from JLab who kindly providing information and advice for this paper. We particularly acknowledge S. Kim for his original SUPERFISH study on this subject.

References

[1] H. Padamsee, et al., *RF Superconductivity for Accelerators*, John Wiley & Sons, INC. (1998), pp. 129-143.

[2] T. E. Mason, "The Spallation Neutron Source: A Powerful Tool for Materials Research," PAC2001, Chicago, IL, June 2001.

[3] I. E. Campisi, et al., "The Fundamental Power Coupler Prototype for the Spallation Neutron Source (SNS) Superconducting Cavities", PAC2001, Chicago, IL, U.S.A, p.1140 (2001).

[4] J. Wei, et al., Design Ptimization and the Path towards a 2 MW Spallation Neutron Source", PAC2001, Chicago, IL, p. 319 (2001).

[5] E. Haebel, "Couplers, Tutorial and Update", Particle Accelerators, Vol. 40, pp.141-159 (1992).

[6] R. Beringer, Principle of Microwave Circuits, edited by C. Montbomery et al, McGraw-Hill Book Company, Inc. (1948), p238.

[7] L. B. Mullett, *Perturbation of a Resonator*, UK Atomic Energy Research Establishment, Harwell, Berkshire, 1957, Unclassified A.E.R.E. G/R 853.